Architectural switch in plant photosynthetic membranes induced by light stress

Miroslava Herbstová[a,b,c], Stefanie Tietz[a], Christopher Kinzel[a], Maria V. Turkina[d], and Helmut Kirchhoff[a,1]

[a]Institute of Biological Chemistry, College of Agricultural, Human, and Natural Resource Sciences, Washington State University, Pullman, WA 99164; [b]Department of Photosynthesis, Institute of Plant Molecular Biology, Biology Center, Academy of Sciences of the Czech Republic, 370 05, České Budějovice, Czech Republic; [c]Faculty of Science, University of South Bohemia, 370 05 České Budějovice, Czech Republic; and [d]Department of Clinical and Experimental Medicine, Linköping University, SE-581 85 Linköping, Sweden

Edited by Eva-Mari Aro, University of Turku, Turku, Finland, and accepted by the Editorial Board October 17, 2012 (received for review August 20, 2012)

Unavoidable side reactions of photosynthetic energy conversion can damage the water-splitting photosystem II (PSII) holocomplex embedded in the thylakoid membrane system inside chloroplasts. Plant survival is crucially dependent on an efficient molecular repair of damaged PSII realized by a multistep repair cycle. The PSII repair cycle requires a brisk lateral protein traffic between stacked grana thylakoids and unstacked stroma lamellae that is challenged by the tight stacking and low protein mobility in grana. We demonstrated that high light stress induced two main structural changes that work synergistically to improve the accessibility between damaged PSII in grana and its repair machinery in stroma lamellae: lateral shrinkage of grana diameter and increased protein mobility in grana thylakoids. It follows that high light stress triggers an architectural switch of the thylakoid network that is advantageous for swift protein repair. Studies of the thylakoid kinase mutant *stn8* and the double mutant *stn7/8* demonstrate the central role of protein phosphorylation for the structural alterations. These findings are based on the elaboration of mathematical tools for analyzing confocal laser-scanning microscopic images to study changes in the sophisticated thylakoid architecture in intact protoplasts.

confocal microscopy | macromolecular crowding | photosynthesis

Photosynthetic transformation of sunlight into metabolic energy equivalents is a dangerous venture, because toxic side products of the primary photochemical processes can lead to uncontrolled damage. Harmful photosynthetic side reactions cannot be avoided completely and become a serious problem under stress (e.g., high light stress). The main target of photoinhibition (PI) is the D1 subunit of the water-splitting photosystem II (PSII) (1, 2). The D1 subunit is buried in the massive (1,400 kDa) PSII holocomplex that is organized as a dimer and binds between two and four trimeric light-harvesting complex IIs (LHCIIs) (3, 4). Estimates predict that without repair of damaged PSII, the efficiency for photosynthetic energy conversion would drop below 5% (5). Consequently, plants would not survive in a highly dynamic and competitive natural environment. Plants address this challenge through the evolutionary invention of one of the fastest and most efficient molecular repair mechanisms in nature, the PSII repair cycle (5–7).

The PSII repair cycle consist of a series of events, including phosphorylation/ dephosphorylation of PSII subunits, holocomplex disassembly/reassembly, and D1 degradation/de novo synthesis (8–10). All of these reactions are harbored in or at the thylakoid membrane system inside the chloroplast. The complex folding of the thylakoid membrane leads to a structural differentiation into stacked grana regions interconnected by unstacked stroma lamellae (11–13). This structural heterogeneity is accompanied by, and partly driven by, differential protein distributions. PSII and LHCII are concentrated in grana stacks, photosystem I (PSI) and the ATPase are more abundant in stroma lamellae, whereas the cytochrome (cyt) b_6f complex is assumed to be distributed homogenously (14–16).

An important consequence of the thylakoid architecture is the spatial lateral separation (up to a few 100 nm) of PSII in grana thylakoids from its repair machinery localized mainly in the stroma lamellae. Thus, restoration of damaged PSII requires that proteins travel from stacked to unstacked thylakoid regions and back. An unsolved problem is that protein traffic through grana membranes is challenged by macromolecular crowding, which severely limits the mobility of the PSII holocomplex (17). Diffusion measurements by the fluorescence recovery after photobleaching (FRAP) technique have shoun that only 15–25% of the protein complexes in grana are mobile (18, 19). Furthermore, this mobile fraction most likely represents the much smaller LHCII, not PSII. Immobility of the PSII holocomplex in grana is supported by computer simulations (20). Knowledge of how damaged PSII in grana is mobilized to enter the repair process is essential to understanding how plants maintain their photosynthetic performance.

Two factors could facilitate lateral diffusion of damaged PSII through crowded grana, both of which are triggered by phosphorylation of PSII subunits (D1, D2, CP43, and psbH), mainly by the *stn8* kinase (8, 9, 21, 22) and eventually also by the *stn7* kinase (23). One of these factors is disassembly of the dimeric holocomplex to a smaller monomeric unit. Although evidence indicates that PI leads to phosphorylation-dependent dismantling of the PSII holocomplex (23, 24), the consequences for PSII mobility are less clear. For example, the correlation between particle size and particle mobility in crowded grana is difficult to predict. Although it seems intuitively attractive that smaller proteins move faster, the opposite effect has been demonstrated by Monte Carlo computer simulation for stacked grana (25). The other factor that may contribute to mobilization of damaged PSII is partial destacking of the grana. The grana system can alter its overall shape in response to environmental conditions (26–28). Evidence exists that PI leads to a partial destacking of grana (29, 30); however, this could mean either a transversal increase of the stromal gap between adjacent membranes in a granum (a so-called "partition") or a lateral decrease in the diameter of a grana stack. Although the literature favors the first possibility, information on changes in grana diameter is limited.

In this study, we used unique combinations of confocal laser scanning microscopy (CLSM) and mathematical image analysis to study structural changes of the grana arrangement in intact protoplasts induced by high-light (HL) treatment. These structural studies were complemented by compositional analysis of

Author contributions: H.K. designed research; M.H., S.T., C.K., M.V.T., and H.K. performed research; M.H., S.T., C.K., M.V.T., and H.K. analyzed data; and M.H. and H.K. wrote the paper.

The authors declare no conflict of interest.

This article is a PNAS Direct Submission. E.-M.A. is a guest editor invited by the Editorial Board.

[1]To whom correspondence should be addressed. E-mail: kirchhh@wsu.edu.

This article contains supporting information online at www.pnas.org/lookup/suppl/doi:10.1073/pnas.1214265109/-/DCSupplemental

isolated stroma lamellae and protein diffusion measurements by FRAP on isolated grana thylakoids. Our results reveal that HL treatment leads to reduced grana diameter and condensation of the grana network, along with increased mobility of grana-hosted protein complexes. Measurements on *stn8* and *stn7/8* double mutants also revealed that phosphorylation of PSII and LHCII subunits are involved in these changes.

Results

Protoplasts for Studying Photoinhibition of PSII. High light stress in plants has so far been studied in leaves, isolated chloroplasts, and thylakoid membranes (21, 29, 31). In this paper, we report this phenomenon in detail using protoplasts isolated from *Arabidopsis thaliana*. An advantage of this approach for HL studies is that the light distribution is more uniform in protoplasts than in leaves, which have complex and variable optical properties, allowing homogeneous inhibition of the PSII complexes in the sample. Furthermore, the accessibility and distribution of effectors, such as inhibitors, is better and more homogeneous in protoplasts. For example, inhibition of plastidial protein synthesis requires several hours of incubation in a lincomycin solution and/or vacuum infiltration (30, 32), which can be avoided by using protoplasts (*Materials and Methods*). Protoplasts also can be used directly for CLSM studies, allowing for fast and easy isolation of thylakoid membranes and their subfragments. In the present study, we demonstrated the successful preparation of grana thylakoids and stroma lamellae from protoplasts by monitoring 77 K fluorescence spectra and using SDS/PAGE (Fig. S1).

HL treatment of protoplasts was characterized by changes in the ratio of variable chlorophyll fluorescence (F_v) to maximal chlorophyll fluorescence (F_{max}) and by D1 protein content in the presence or absence of lincomycin (Fig. S2). The F_v/F_{max} ratio decreased to ~55% after 60 min of HL treatment. The decrease was faster in lincomycin-treated protoplasts, with ~35% decrease after 60 min, demonstrating that impaired protein synthesis in chloroplasts increases the risk of PSII photodamage. This is indicative of an operative PSII repair cycle in protoplasts, as was further confirmed by measurements of D1 content derived from Western blot analysis (Fig. S2, *Inset*). In the presence of lincomycin, D1 was rapidly degraded, but its content remained almost unchanged over 60 min of HL treatment in the absence of the inhibitor. The unchanged D1 level without lincomycin is the result of a balanced D1 degradation and de novo synthesis by the PSII repair cycle. Overall, the characteristics of HL-induced PSII inactivation and D1 degradation in protoplasts were similar to those seen in leaves (24).

Structural Changes in the Thylakoid Membrane Network Induced by PI. Architectural changes in the overall thylakoid organization of protoplasts in the absence of lincomycin were studied by CLSM in combination with mathematical analysis. The intactness of protoplasts used for these measurements was verified by checking the integrity of the cytoplasm membranes stained with the membrane marker boron-dipyrromethene (BODIPY) (Fig. 1*A*). For morphometric analysis, chloroplasts in protoplasts were selected in which grana were oriented in a top view position, where they appear circular. The first analysis concerned the overall arrangement of grana in thylakoids, that is, quantification of the separation between adjacent grana stacks by next-neighbor distribution analysis (Fig. 1*B*). The Cartesian coordinates of the center of individual grana stacks were extracted (Fig. 1*B*), leading to *x,y* maps of grana positions. From these maps, the next-neighbor distribution function (NNDF) was calculated (Fig. 1*B*, *Right*). NNDF analysis of WT cells showed that the distance between adjacent grana stacks was reduced by ~25% in HL-treated protoplasts, indicating condensation of the entire grana network. This condensation occured within the first 30 min of HL treatment (Fig. 1*B*); no further condensation was apparent at longer time points. In contrast to WT cells, no HL-induced reduction in grana–grana separation was seen in *stn8* or *stn7/8* mutants (Fig. 1*B*).

The second morphometric analysis concerns the grana diameter that was determined from gray-scale profiles of individual grana stacks (Fig. 1*C*). The grana image gallery in Fig. 1*C* shows a decrease in grana diameter after 30 min of illumination. This was quantified by measuring the FWHM values derived from the gray-scale profiles. Note that FWHM values were well above the CLSM's lateral resolution of 288 nm (Fig. S3), but optical blurring effects were apparent in this size range, causing widening of the measured diameter. This was corrected by a deconvolution procedure (Fig. S3). The corrected values for WT protoplasts shown in Fig. 1*C* (*Right*) show lateral shrinkage of grana diameter from ~370 nm to ~300 nm after HL. This shrinkage occurred within the first 30 min of HL treatment; after this time point, grana diameter remained unchanged. The reduction in grana diameter derived from CLSM image analysis was confirmed by biochemical fractionation data quantifying the percentage of grana thylakoid membranes (Fig. 1*C*, *Right*). After thylakoid fractionation with digitonin into grana and stroma

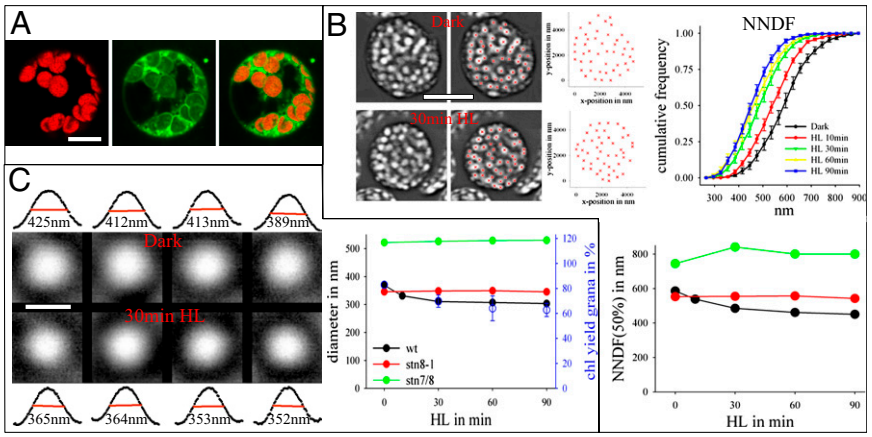

Fig. 1. Architectural changes in thylakoid membranes in protoplasts from WT, *stn8*, and *stn7/8* mutants induced by HL treatment. (*A*) CLSM images of protoplasts. Red indicates the natural chlorophyll autofluorescence; green, BODIPY fluorescence (stains biomembranes). Both images are merged on the right. (Scale bar: 10 μm.) (*B*) NNDF analysis of the grana network in dark-adapted and HL-treated (30 min) samples. (*Left*) CLSM examples showing chlorophyll fluorescence. (Scale bar: 4 μm.) (*Upper Right*) Cartesian coordinates of the center of gravity for the grana stacks were extracted from the CLSM images of protoplasts in *A* (red crosses) and analyzed by NNDF. Data are mean ± SE, collected from three independent preparations. (*Lower Right*) Mean grana–grana separation distances, quantified as the distance at which the NNDF is 50%, derived from the NNDF analysis. The color code is as in *C*. (*C*) (*Left*) Gallery of grana discs for WT samples. Gray-scale profiles (curves at the top and bottom) were extracted from CLSM micrographs of individual grana discs, and FWHM values were determined (red lines and numbers). (Scale bar: 500 nm.) (*Right*) FWHM as a function of the incubation time under HL treatment for WT (black), *stn8* (red), and *stn7/8* double mutant (green). Data were corrected for blurring effects as described in Fig. S3. Blue circles indicate the yield of grana membranes after digitonin fragmentation of thylakoids isolated from protoplasts. The yield is defined as the total chlorophyll content of grana relative to the content of grana plus stroma lamellae.

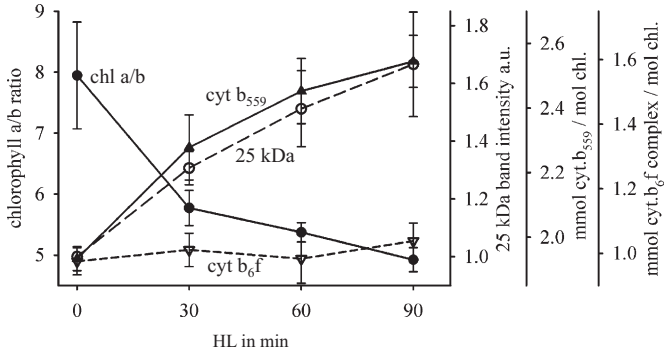

Fig. 2. Compositional changes of isolated stroma lamellae induced by HL treatment. The intensity of the 25-kDa band from SDS/PAGE gels (Fig. S1*A*) is a measure of LHCII content (open circles) and cyt *b559* of PSII (solid triangles). Solid circles indicate chl a/b ratio. The cyt b_6f complex was quantified by averaging cyt *f* and cyt b_6 contents (open triangles). Data are mean ± SE of three independent preparations.

lamellae, the percentage of chlorophyll found in the grana fraction decreased from ∼83% in dark-adapted samples to ∼66% in HL-treated samples, indicating grana destacking (Fig. 1*C*, *Right*). This was in accordance with previous biochemical data (29). Both grana shrinkage and grana network condensation had a half time of approximately 10 min (Fig. 1). The architectural changes in the thylakoid system were not caused by shrinkage of the overall chloroplast, as indicated by unaltered chloroplast sizes measured by CLSM. The chloroplast areas of dark-adapted, 30-min HL-treated, 60-min HL-treated, and 90-min HL-treated samples were 27.9 ± 1.8 μm^2 ($n = 74$), 26.6 ± 1.9 μm^2 ($n = 61$), 28.2 ± 1.7 μm^2 ($n = 59$), and 25.3 ± 1.3 μm^2 ($n = 54$), respectively. Furthermore, grana diameter was approximately 50% larger in the *stn7/8* double mutant compared with the dark-adapted WT samples (Fig. 1*C*, *Right*), in agreement with EM studies (30). In contrast to the EM studies, however, no such increase was observed for *stn8*. We have no explanation for this discrepancy. However, similar to the NNDF analysis, HL-induced shrinkage of the grana diameter was not apparent for both the *stn8* and *stn7/8* double mutants (Fig. 1*C*).

Transformation of stacked to unstacked thylakoid membranes is expected to be accompanied by the release of grana-hosted proteins to stroma lamellae. To test this, we characterized the compositional changes of isolated stroma lamellae using spectroscopic and gel electrophoresis methods (Fig. 2). HL treatment led to a drop in the chlorophyll a/b ratio from ∼8 in dark-adapted samples to ∼5 after 90 min of HL treatment, indicating increased LHCII content in stroma lamellae. This observation was confirmed by densitometric analysis of the 25-kDa band on SDS/PAGE (Fig. 2 and Fig. S1*A*). We also observed a progressive increase in PSII content in stroma lamellae determined by quantification of the cyt *b559* concentration (Fig. 2). Cyt *b559* is found exclusively in the PSII core and thus is a marker for the content of this photosystem. The PSII concentration, expressed as cyt *b559*/chlorophyll ratio, increased by ∼30% after the 90-min HL treatment. Accumulation of PSII in stroma lamellae is further supported by Western blot data on isolated stroma lamellae showing a continuous increase in D1 content over the 90-min HL treatment (Fig. S1*B*). The increases in LHCII and PSII are in agreement with the increase in fluorescence emission around the 684-nm band (F684) detected in the 77 K fluorescence spectra of isolated stroma lamellae (Fig. S1*D*). These in vitro studies are supported by CLSM measurements with intact protoplasts showing increasing intensity of the fluorescence preferentially emitted from PSII and LHCII in stroma lamellae after HL treatment (Fig. S4). PSII and LHCII content in unstacked thylakoid membranes increased steadily during the 90-min HL treatment (Fig. 2 and Fig. S1). Partial lateral destacking can explain this increase only for the first 30 min (Fig. 1*C*). The further increase beyond 30 min suggests a diffusion of grana-hosted proteins out of the stacked thylakoid regions, as discussed in the next section. Finally, quantification of the cyt b_6f content in stroma lamellae revealed almost no change (Fig. 2), consistent with data showing a homogenous distribution of this complex between stacked and unstacked thylakoids (14, 15).

Diffusion Analysis by FRAP in Isolated Grana Membranes. For measuring diffusion of chlorophyll-binding protein complexes (PSII and LHCII) in grana, we used FRAP for digitonin-prepared grana thylakoids, as described previously in isolated grana prepared by treatment with Triton X100 (*BBY* particles) (18). In contrast to *BBY* membranes, the grana membranes isolated by digitonin treatment still contained the cyt b_6f complex. From difference spectroscopic measurements of cyt *f* and cyt b_6, we determined a chlorophyll/cyt b_6f complex ratio of 1,362 ± 73 ($n = 5$), indicating a more native membrane state compared with *BBY* membranes (14–16). FRAP data are summarized in Fig. 3. At time point 0, a thin line of pigments in the middle of a grana patch was bleached, and the time-dependent fluorescence recovery was recorded. Greater fluorescence recovery indicates a higher fraction of mobile chlorophyll–protein complexes. The FRAP data reveal significantly increased protein mobility in grana thylakoids isolated from WT protoplasts after HL treatment in the absence of lincomycin. Under non-photoinhibiting conditions, ∼24% of grana protein complexes were mobile, whereas after HL treatment, the mobile fraction increased to ∼40% (Fig. 3, *Inset*). Our findings indicate that protein mobility in grana membranes is greater after HL incubation, in accordance with data showing greater protein exchange between grana discs after HL treatment (19). Similar to the changes in grana diameter (Fig. 1*C*), the increase in protein mobility leveled off after 30 min. This increased protein mobility was not observed for the kinase mutants (Fig. 3, *Inset*), indicating that phosphorylation in grana is required for protein mobilization.

Discussion

The data reported here indicate that high light stress induces an architectural switch of the entire thylakoid network in chloroplasts to a state advantageous for the repair of damaged PSII (Fig. 4). The two main features of this switch are partial lateral destacking of grana and increased protein mobility in grana core

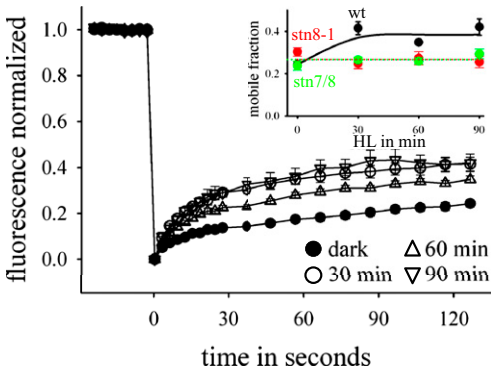

Fig. 3. FRAP analysis of isolated grana membranes. At time 0, chlorophyll fluorescence was irreversibly bleached in grana, and time-dependent recovery was monitored in dark-adapted samples and HL-treated samples. (*Inset*) Mobile fraction for the different samples of WT and kinase mutants, estimated as the last data point in the recovery kinetics. Data are mean ± SE of 10–21 different grana patches for each time point.

membranes. These changes work synergistically to enhance the accessibility of photoinhibited PSII to its repair machinery and are accompanied by a condensation of the grana network (Fig. 1*B*). More importantly, the comparisons of WT with *stn8* and *stn7*/*8* double mutants clearly indicate that the HL treatment-induced structural alterations and the changes in protein mobility of grana-hosted proteins reported here require phosphorylation of PSII subunits and eventually of LHCII as well (Figs. 2 *B* and *C* and 4, *Inset*).

Our findings demonstrate that HL treatment causes lateral shrinkage of grana discs. Previous studies reported partial destacking of grana induced by HL treatment (29, 33), but the biochemical fractionation/light-scattering approaches used in those studies did not allow discrimination between an increase in the partition gap and a reduction in grana diameter. Fristedt et al. (30) also used EM to study changes in thylakoid ultrastructure induced by HL treatment and reported no differences in grana diameter, in contrast to our findings; however, the error bars for determination of the grana diameter from the EM micrographs are on the order of ±35%, which does not allow visualization of the more subtle 20% reduction detected by CLSM analysis (Fig. 1*C*). Of note, the reduction in grana diameter does not exclude the possibility that HL also triggers transverse widening of stromal partition gap; as such, it introduces a structural element not considered so far.

An interesting observation is the cessation of grana destacking at a diameter of ∼300 nm (Fig. 1*C*). This is reminiscent of the partial destacking induced by state transition that is operative under low light and controlled by the *stn7* kinase (6, 27, 34). In plants, transition from state 1 to state 2 leads to a reduction of the grana area by up to ∼25% but no further (6), similar to what we found for HL-treated samples (Fig. 1*C*). Although the kinases and target proteins for phosphorylation are different (LHCII subunits for state transitions and PSII core proteins for HL treatment), both processes led to similar degrees of lateral unstacking. This corresponds to the idea that the phosphorylation level of grana proteins is a general determinant of thylakoid membrane stacking (33). The meaning of a limiting "lateral destacking threshold" remains to be elucidated, but points to structural and compositional differences within the grana, that is, between core grana and peripheral grana. This is in line with the hypothesis that grana margins form a functional domain for the PSII repair cycle (35), which allows for efficient contact between damaged PSII and its repair machinery.

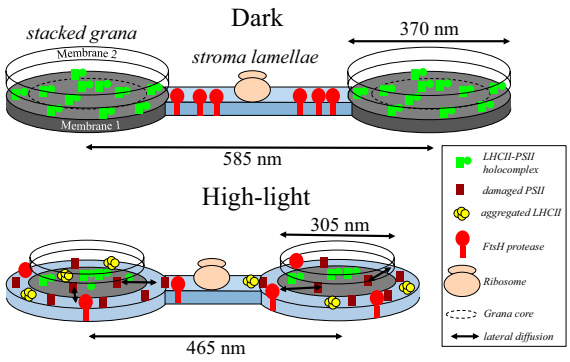

Fig. 4. Cartoon summarizing HL treatment-induced architectural changes in thylakoids. The stromal gap between stacked grana discs is too narrow to allow access of FtsH proteases and ribosomes. Under HL treatment, lateral partial destacking of grana and increased protein mobility of grana-hosted proteins renders damaged PSII accessible for its repair machinery in unstacked thylakoid membranes. For clarity, membrane 2 is left open.

Partial destacking by shrinkage of the grana diameter leads to the release of former grana-hosted proteins, including PSII and LHCII (Fig. 2 and Fig. S1*D*). The functional state of the released LHCII in stroma lamellae is critical, because free LHCII can produce toxic reactive oxygen species. For the green algae *Chlamydomanos reinhardtii,* it was shown that under state II, phospho-LHCII that uncouples from PSII switches to an energy-dissipative state, likely by formation of small aggregates (36). This switch safely converts harvested energy into heat. In contrast to state transitions, the LHCII phosphorylation level is lower in HL-treated samples compared with dark-adapted samples (33), because the *stn7* kinase is turned off in high light (21, 37, 38). This was apparent for thylakoids isolated from HL-illuminated protoplasts (Fig. S5*A*). However, the phosphorylation level was 50–80% higher in isolated stroma lamellae compared with their dark-adapted counterparts (Figs. S4*B* and S5*A*, *Left*), in accordance with previous results (39). Thus, it is likely that phospho-LHCII localized in unstacked thylakoids of HL-illuminated protoplasts is in a quenched state, as reported for *Chlamydomonas*.

To obtain functional information about LHCII in isolated grana and stroma lamellae, we analyzed PSII/LHCII-specific changes in fluorescence spectra recorded at 77 K (Fig. S6). For grana isolated from HL-treated samples, new emission bands at ∼680 nm and ∼700 nm indicated dissociation of LHCII from PSII and partial LHCII aggregation (∼700-nm band). Analysis of fluorescence spectra for stroma lamellae revealed an increase in aggregated quenched LHCII and a decrease in free unquenched LHCII (Fig. S6). This indicates that the LHCII released to the stroma lamellae by partial destacking is in an energy-quenched state. The mechanism behind the switch of trimeric phospho-LHCII to a dissipative state in stroma lamellae is unclear, but it supports photoprotection under light stress by lowering the excitation pressure on the photosystems and by minimizing reactive oxygen species production.

Lateral partial destacking enables direct access to the repair machinery in the stroma lamellae, but only for those PSII complexes localized in the destacked peripheral grana region. Although this is a considerable PSII fraction (∼30–40%, estimated by assuming a homogenous PSII distribution in stacked grana), the fate of PSII complexes damaged in the core part of the grana not subjected to destacking is unclear. These PSII complexes can escape from stacked grana only by lateral diffusion. The FRAP data show that protein mobility in isolated grana thylakoids increased significantly after HL treatment (Fig. 3). Thus, HL stress switched the stacked membranes to a more fluid state that eventually allowed damaged PSII to escape from this thylakoid region. Consistent with this view was the increase in PSII (cyt *b559*) and LHCII (25-kDa band) concentrations in stroma lamellae after 30 min of HL treatment (Fig. 2). This increase at later time points cannot be explained by lateral destacking (no further destacking after 30 min; Fig. 1*C*), but can be understood by diffusion-dependent migration of proteins from the grana core region. Consequently, HL treatment apparently causes a net efflux of PSII from stacked grana, as indeed has been confirmed by EM on freeze-fractured thylakoids (19).

Lateral destacking has several implications for the PSII repair cycle (Fig. 4). First, a reduction in grana diameter allows damaged PSII localized in the destacked grana region to reach its repair machinery in unstacked thylakoid membranes without long-range diffusion through crowded grana. Second, lateral destacking reduces the diffusion path and consequently the diffusion time for PSII complexes that are photoinhibited in the remaining stacked grana core region. Based on the measured changes in grana diameter (Fig. 1*C*), it follows that the mean diffusion path for proteins in stacked grana (i.e., the path for 50% of grana PSII) was reduced from 131 nm in the dark to 108 nm after 30 min of HL treatment (i.e., by ∼20%). Another

geometric impact of reduced grana diameter for mass flow out of the grana is the increase in the grana perimeter-to-area ratio. This leads to an increase in protein exchange zones at the stacked–unstacked interface, which is advantageous for lateral membrane traffic of damaged and repaired PSII.

Third, the release of damaged PSII into unstacked regions allows direct physical contact to hexameric FtsH proteases that degrades the D1 subunit (40). The height of the stromal protrusion of the FtsH proteases is 6.5 nm (41). This large protrusion may exclude the FtsH proteases from stacked regions by steric hindrances, because ultrastructural data showed an only 3- to 4-nm wide partition gap in grana (26, 42). Intermixing of FtsH proteases and photoinhibited PSII by partial lateral destacking is favorable for a swift D1 degradation, as postulated recently (43, 44).

Finally, the release of LHCII from grana is a mechanism to lower the excitonic pressure of active PSII complexes in the remaining stacked grana area. Any LHCII remaining in core grana could serve as a light harvester for nondamaged PSII, which would be counterproductive for protecting the photosynthetic machinery under HL stress.

Consequences of grana network condensation (Figs. 1*B* and 4) for PSII repair are less clear. A possible advantage is that the mean distance between the rim of stacked grana to proteins in stroma lamellae is reduced by condensation, which could speed diffusion- dependent processes in unstacked thylakoid regions. With respect to the PSII repair cycle, affected processes include interactions between phosphorylated damaged PSII and its phosphatase(s), between dephosphorylated PSII and FtsH proteases, and between PSII and ribosomes for cotranslational insertion of de novo synthesized D1 subunits, as well as the back-transfer of reassembled repaired PSII to grana. Knowledge of protein diffusion in unstacked thylakoid regions is limited to grana end membranes (45) and the exchange between grana-separated stroma lamellae (46). Protein mobility is expected to be higher in stroma lamellae than in grana thylakoids, because of a lower protein-packing density (15, 47). The protein-packing density in stroma lamellae is significant, however. The protein: lipid (wt/wt) ratio is 86:14 for grana and 61:39 for stroma lamellae (47). Furthermore, HL treatment led to an increase in protein concentration in unstacked thylakoid membranes (Fig. 2). Thus, the reduction of the diffusion path between stacked and unstacked regions by condensation of the grana network could facilitate the identification of reaction partners involved in the multistep repair process in stroma lamellae.

The folding of the thylakoid membrane system to strictly stacked grana sets constraints on protein exchange between stacked and unstacked membrane regions. In contrast, brisk protein traffic between these subcompartments is required for the repair of damaged PSII as well as other adaptation processes, such as state transitions or remodeling of protein composition in the course of long-term acclimations. The architectural switch of the thylakoid membrane system reported in this study is an elegant way of enhancing the multiple diffusion-dependent reactions involved in the PSII repair cycle.

Materials and Methods

Protoplast Preparation. WT *A. thaliana* (ecotype Columbia) plants were grown in soil (9 h, 100 μmol quanta·m^{-2}·s^{-1}, 15 h dark) at 20 °C in a growth chamber. Protoplasts were isolated as described previously (48). In brief, leaves from 4- to 6-wk-old plants were cut into small pieces and incubated in protoplast buffer [20 mM MES (pH 5.7), 0.5 M mannitol, 10 mM $CaCl_2$, 10 mM KCl] supplemented with 1% (wt/vol) cellulase and 1% (wt/vol) maceroenzyme overnight at 15 °C in an incubator shaker (Inova 4403; New Brunswick). Protoplasts were collected by filtering through 80-μm Miracloth, then centrifuged at 150 × *g* for 3 min at 4 °C. The protoplast pellet was then resuspended in protoplast buffer (pH 7.4). Because the dependence of grana stacking on divalent cation concentrations is rather insensitive at concentrations above 2 mM, incubation in protoplast buffer (10 mM $CaCl_2$) was expected to have no significant effect on stacking behavior (49, 50).

HL Treatment of Protoplasts. Protoplasts at a chlorophyll concentration of 0.2 mg·mL^{-1} were illuminated for 10, 30, 60, and 90 min with cold white light at ~2,000 μmol photons·m^{-2}·s^{-1} (Leica KL1500LED) at 20 °C. Control samples were kept in the dark under otherwise identical conditions. The maximal photochemical efficiency of PSII was measured as F_v/F_{max} with a pulse-modulated fluorimeter (Hansatech OxyLab). For inhibition of D1 de novo synthesis, protoplasts were treated for 15 min in the dark with 0.25 M lincomycin (Sigma-Aldrich). Lincomycin treatment did not affect the F_v/F_{max} ratio of dark-adapted samples.

Isolation and Thylakoid Membrane Subfractions. Thylakoid membranes were obtained by pottering intact protoplasts in a hypotonic buffer containing 40 mM Hepes (pH 7.6), 80 mM KCl, 7 mM $MgCl_2$, and the protease inhibitors Pefablock SC (Roche), leupeptin, and antipain (Sigma-Aldrich). Thylakoids were pelleted (at 3,200 × *g* for 10 min at 4 °C) and resuspended in a storage buffer containing 50 mM Hepes (pH 7.5), 0.1 M sorbitol, and 2 mM $MgCl_2$. Thylakoids were subfractionated into grana and stroma lamellae by digitonin treatment, followed by differential centrifugation as described by Fristedt (30). Chlorophyll concentration was determined spectroscopically in 80% (vol/vol) acetone (51).

CLSM and Image Processing. For CLSM analysis, protoplasts in protoplast buffer (pH 7.2) were stained with BODIPY C12 (Molecular Probes) under anaerobic conditions established by a glucose/glucose-oxidase system (18). Anaerobiosis ensures a stable and high fluorescence signal. Images were obtained with a Leica SP5 microscope. Chlorophyll and BODIPY fluorescence, excited by a 488-nm argon laser line, were detected at 650–720 nm and 510–560 nm, respectively. Images were obtained at a scan rate of 1,000 Hz and a resolution of 1,024 × 1,024 pixels. Four images were averaged to improve the signal-to-noise ratio.

Image analysis and statistical analysis were performed using ImagePro (Media Cybernetics Inc.) and SigmaPlot11 (Systat Software Inc.) software. Grana diameter was determined from gray-scale profiles of individual grana stacks (Fig. 1*C*) and quantified as FWHM. In some cases, the grana shapes are not perfectly round, owing to a slightly staggered arrangement of two grana discs localized in different *z*-planes. To take this into account, only the smallest diameters of these particles were analyzed. The diameter values were corrected by measuring the microscope's point spread function (Fig. S3) using red (660-nm emission) fluorescence microspheres with a diameter of 0.175 ± 0.005 μm (PS-Speck Microscopy Point Source Kit; Invitrogen). The distribution of grana stacks within chloroplasts was characterized by NNDF as described previously (20).

FRAP Measurements. Isolated grana membranes incubated under anaerobic conditions were placed on a glass slide covered with a bilayer of phosphatidylcholine stained with BODIPY C12 (18), to avoid artificial glass–membrane interactions. The incubation buffer contained 30% (wt/vol) Ficoll to reduce the mobility of the small grana membranes. Chlorophyll fluorescence was excited at 488 nm and detected at 650–720 nm. The FRAP approach assumes that the bleached pigments are irreversibly bleached; to test this, whole grana patches were bleached so that no reservoirs of unbleached pigments remained. The recovery of these totally bleached samples was very low (1–3%). The data were corrected against total bleach recovery. FRAP images were analyzed with ImagePro and SigmaPlot software as described previously (18).

Spectroscopy. Low-temperature (77 K) fluorescence emission spectra were recorded with a Horiba Jobin Yvon FluoroMax 4 spectrofluorimeter in the spectral range of 650–800 nm (slit width, 2 nm) with an excitation wavelength of 435 nm (slit width, 5 nm). PSII content was measured by difference spectroscopic quantification of cyt *b559*, and the content of the cyt b_6f complex was measured by quantification of cyt *f* and cyt b_6, as described previously (52). Signals were recorded with a Hitachi U3900 spectrometer (spectral range, 540–575 nm; 2-nm slit width). The spectra were analyzed as described previously (52). Cytochrome concentrations are expressed in mol of cytochrome per mol of chlorophyll.

Electrophoresis and Immunoblot Analysis. Protein composition was determined by SDS/PAGE on 12.5% polyacrylamide gel containing 6 M urea (53) using Coomassie blue staining. Gels were loaded on the chlorophyll basis. For immunoblot analyses, proteins separated by SDS/PAGE were electrotransferred on PVDF membrane (Millipore) as described by Towbin et al. (54). Membranes were probed with antibody raised against C terminus of the D1 protein (Agrisera), then incubated with HRP-conjugated secondary antibody. Immunodecorated bands were detected by fluorography using an

ECL detection kit (GE Healthcare). D1 content was determined form densitometric quantification of the Western blot bands using ImagePro Plus software. Phosphorylation of LHCII in isolated stroma lamellae and intact thylakoids was studied with antithreonine antibodies from Zymed Laboratories as described previously (30).

ACKNOWLEDGMENTS. We thank Dr. Dario Leister for providing seeds of *stn8-1* and *stn7/8* mutants. This research was supported by the Washington State Agricultural Research Center, National Science Foundation Grant MCB-1158571, United States–Israel Binational Agricultural Research and Development Fund Grant US-4334-10, and Development Fund Grant US-4334-10 (all to H.K.); and by institutional support RV:60077344 (to M.H.).

1. Ohad I, Kyle DJ, Arntzen CJ (1984) Membrane protein damage and repair: Removal and replacement of inactivated 32-kilodalton polypeptides in chloroplast membranes. *J Cell Biol* 99(2):481–485.
2. Rokka A, Suorsa M, Saleem A, Battchikova N, Aro EM (2005) Synthesis and assembly of thylakoid protein complexes: Multiple assembly steps of photosystem II. *Biochem J* 388(Pt 1):159–168.
3. Caffarri S, Kouřil R, Kereïche S, Boekema EJ, Croce R (2009) Functional architecture of higher plant photosystem II supercomplexes. *EMBO J* 28(19):3052–3063.
4. Kouřil R, Dekker JP, Boekema EJ (2012) Supramolecular organization of photosystem II in green plants. *Biochim Biophys Acta* 1817(1):2–12.
5. Melis A (1999) Photosystem-II damage and repair cycle in chloroplasts: What modulates the rate of photodamage? *Trends Plant Sci* 4(4):130–135.
6. Kyle DJ, Ohad I, Arntzen CJ (1984) Membrane protein damage and repair: Selective loss of a quinone-protein function in chloroplast membranes. *Proc Natl Acad Sci USA* 81(13):4070–4074.
7. Mulo P, Sirpiö S, Suorsa M, Aro EM (2008) Auxiliary proteins involved in the assembly and sustenance of photosystem II. *Photosynth Res* 98(1-3):489–501.
8. Tikkanen M, Aro EM (2012) Thylakoid protein phosphorylation in dynamic regulation of photosystem II in higher plants. *Biochim Biophys Acta* 1817(1):232–238.
9. Pesaresi P, Pribil M, Wunder T, Leister D (2011) Dynamics of reversible protein phosphorylation in thylakoids of flowering plants: The roles of STN7, STN8 and TAP38. *Biochim Biophys Acta* 1807(8):887–896.
10. Kato Y, Sakamoto W (2009) Protein quality control in chloroplasts: A current model of D1 protein degradation in the photosystem II repair cycle. *J Biochem* 146(4):463–469.
11. Austin JR, 2nd, Staehelin LA (2011) Three-dimensional architecture of grana and stroma thylakoids of higher plants as determined by electron tomography. *Plant Physiol* 155(4):1601–1611.
12. Daum B, Kühlbrandt W (2011) Electron tomography of plant thylakoid membranes. *J Exp Bot* 62(7):2393–2402.
13. Nevo R, Chuartzman SG, Tsabari O, Reich Z (2009) Architecture of thylakoid membrane networks. *Lipids in Photosynthesis: Essential and Regulatory Functions*, eds Wada H, Murata N (Springer, Dordrecht, The Netherlands), pp 295–328.
14. Cox RP, Andersson B (1981) Lateral and transverse organization of cytochromes in the chloroplast thylakoid membrane. *Biochem Biophys Res Commun* 31:1336–1342.
15. Staehelin LA, van der Staay GWM (1996) Structure, composition, functional organization and dynamic properties of thylakoid membranes. *Oxygenic Photosynthesis: The Light Reactions*, eds Ort DA, Yocum CF (Kluwer, Dordrecht, The Netherlands), pp 11–30.
16. Albertsson P (2001) A quantitative model of the domain structure of the photosynthetic membrane. *Trends Plant Sci* 6(8):349–358.
17. Kirchhoff H (2008) Molecular crowding and order in photosynthetic membranes. *Trends Plant Sci* 13(5):201–207.
18. Kirchhoff H, Haferkamp S, Allen JF, Epstein D, Mullineaux CW (2008) Significance of macromolecular crowding for protein diffusion in thylakoid membranes of chloroplasts. *Plant Physiol* 146:1571–1578.
19. Goral TK, et al. (2010) Visualizing the mobility and distribution of chlorophyll proteins in higher plant thylakoid membranes: Effects of photoinhibition and protein phosphorylation. *Plant J* 62(6):948–959.
20. Kirchhoff H, Tremmel I, Haase W, Kubitscheck U (2004) Supramolecular photosystem II organization in grana thylakoid membranes: Evidence for a structured arrangement. *Biochemistry* 43(28):9204–9213.
21. Bonardi V, et al. (2005) Photosystem II core phosphorylation and photosynthetic acclimation require two different protein kinases. *Nature* 437(7062):1179–1182.
22. Vainonen JP, Hansson M, Vener AV (2005) STN8 protein kinase in *Arabidopsis thaliana* is specific in phosphorylation of photosystem II core proteins. *J Biol Chem* 280(39): 33679–33686.
23. Fristedt R, Vener AV (2011) High light-induced disassembly of photosystem II supercomplexes in *Arabidopsis* requires STN7-dependent phosphorylation of CP29. *PLoS ONE* 6(9):e24565.
24. Tikkanen M, Nurmi M, Kangasjärvi S, Aro E-M (2008) Core protein phosphorylation facilitates the repair of photodamaged photosystem II at high light. *Biochim Biophys Acta* 1777(11):1432–1437.
25. Tremmel IG, Kirchhoff H, Weis E, Farquhar GD (2003) Dependence of plastoquinol diffusion on the shape, size, and density of integral thylakoid proteins. *Biochim Biophys Acta* 1607(2-3):97–109.
26. Kirchhoff H, et al. (2011) Dynamic control of protein diffusion within the granal thylakoid lumen. *Proc Natl Acad Sci USA* 108(50):20248–20253.
27. Chuartzman SG, et al. (2008) Thylakoid membrane remodeling during state transitions in *Arabidopsis*. *Plant Cell* 20(4):1029–1039.
28. Anderson JM (1988) Thylakoid membrane organization in sun/shade acclimation. *Aust J Plant Physiol* 15:11–26.
29. Khatoon M, et al. (2009) Quality control of photosystem II: Thylakoid unstacking is necessary to avoid further damage to the D1 protein and to facilitate D1 degradation under light stress in spinach thylakoids. *J Biol Chem* 284(37):25343–25352.
30. Fristedt R, et al. (2009) Phosphorylation of photosystem II controls functional macroscopic folding of photosynthetic membranes in *Arabidopsis*. *Plant Cell* 21(12): 3950–3964.
31. Tyystjärvi E, Aro EM (1996) The rate constant of photoinhibition, measured in lincomycin-treated leaves, is directly proportional to light intensity. *Proc Natl Acad Sci USA* 93(5):2213–2218.
32. Pokorska B, Zienkiewicz M, Powikrowska M, Drozak A, Romanowska E (2009) Differential turnover of the photosystem II reaction centre D1 protein in mesophyll and bundle sheath chloroplasts of maize. *Biochim Biophys Acta* 1787(10):1161–1169.
33. Fristedt R, Granath P, Vener AV (2010) A protein phosphorylation threshold for functional stacking of plant photosynthetic membranes. *PLoS ONE* 5(6):e10963.
34. Rochaix JD (2011) Regulation of photosynthetic electron transport. *Biochim Biophys Acta* 1807(3):375–383.
35. Kettunen R, Tyystjärvi E, Aro EM (1995) Do grana margins of thylakoid membranes form a functional domain during repair cycle of photosystem II?. *Photosynthesis: From Light to Biosphere*, ed Mathis P (Kluwer, Dordrecht, The Netherlands), Vol IV, pp 331–334.
36. Iwai M, Yokono M, Inada N, Minagawa J (2010) Live-cell imaging of photosystem II antenna dissociation during state transitions. *Proc Natl Acad Sci USA* 107(5): 2337–2342.
37. Rintamäki E, Martinsuo P, Pursiheimo S, Aro EM (2000) Cooperative regulation of light-harvesting complex II phosphorylation via the plastoquinol and ferredoxin-thioredoxin system in chloroplasts. *Proc Natl Acad Sci USA* 97(21):11644–11649.
38. Rochaix JD (2007) Role of thylakoid protein kinases in photosynthetic acclimation. *FEBS Lett* 581(15):2768–2775.
39. Baena González E, Barbato R, Aro E-M (1999) Role of phosphorylation in the repair cycle and oligomeric structure of photosystem II. *Planta* 208:196–204.
40. Nixon PJ, Michoux F, Yu J, Boehm M, Komenda J (2010) Recent advances in understanding the assembly and repair of photosystem II. *Ann Bot (Lond)* 106(1):1–16.
41. Suno R, et al. (2006) Structure of the whole cytosolic region of ATP-dependent protease FtsH. *Mol Cell* 22(5):575–585.
42. Daum B, Nicastro D, Austin J II, McIntosh JR, Kühlbrandt W (2010) Arrangement of photosystem II and ATP synthase in chloroplast membranes of spinach and pea. *Plant Cell* 22(4):1299–1312.
43. Yoshioka M, et al. (2010) Quality control of photosystem II: FtsH hexamers are localized near photosystem II at grana for the swift repair of damage. *J Biol Chem* 285 (53):41972–41981.
44. Yoshioka M, Yamamoto Y (2011) Quality control of photosystem II: Where and how does the degradation of the D1 protein by FtsH proteases start under light stress? Facts and hypotheses. *J Photochem Photobiol B* 104(1-2):229–235.
45. Consoli E, Croce R, Dunlap DD, Finzi L (2005) Diffusion of light-harvesting complex II in the thylakoid membranes. *EMBO Rep* 6(8):782–786.
46. Vladimirou E, et al. (2009) Diffusion of a membrane protein, Tat subunit Hcf106, is highly restricted within the chloroplast thylakoid network. *FEBS Lett* 583(22): 3690–3696.
47. Murphy DJ (1986) The molecular organisation of the photosynthetic membranes of higher plants. *Biochim Biophys Acta* 864:33–94.
48. Sharpe RM, Mahajan A, Takacs EM, Stern DB, Cahoon AB (2011) Developmental and cell type characterization of bundle sheath and mesophyll chloroplast transcript abundance in maize. *Curr Genet* 57(2):89–102.
49. Staehelin LA (1976) Reversible particle movements associated with unstacking and restacking of chloroplast membranes in vitro. *J Cell Biol* 71(1):136–158.
50. Kirchhoff H, Borinski M, Lenhert S, Chi L, Büchel C (2004) Transversal and lateral exciton energy transfer in grana thylakoids of spinach. *Biochemistry* 43(45): 14508–14516.
51. Porra RJ, Thompson WA, Kriedermann PE (1989) Determination of accurate extinction coefficient and simultaneous equations for essaying chlorophylls a and b extracted with four different solvents: Verification of the concentration of chlorophyll standards by atomic absorption spectroscopy. *Biochim Biophys Acta* 975:384–394.
52. Kirchhoff H, Mukherjee U, Galla HJ (2002) The molecular architecture of the thylakoid membrane: The lipidic diffusion space for plastoquinone. *Biochem* 41:4872–4882.
53. Laemmli UK (1970) Cleavage of structural proteins during the assembly of the head of bacteriophage T4. *Nature* 227(5259):680–685.
54. Towbin H, Staehelin T, Gordon J (1979) Electrophoretic transfer of proteins from polyacrylamide gels to nitrocellulose sheets: Procedure and some applications. *Proc Natl Acad Sci USA* 76(9):4350–4354.